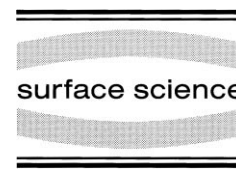




ELSEVIER

Surface Science 433–435 (1999) 119–126



www.elsevier.nl/locate/susc

Density-functional theory study of the catalytic oxidation of CO over transition metal surfaces

C. Stampfl ^{*}, M. Scheffler

Fritz-Haber-Institut der Max-Planck-Gesellschaft, Faradayweg 4–6, D-14195 Berlin-Dahlem, Germany

Abstract

In recent years, due to improvements in calculation methods and increased computer power, it has become possible to perform first-principles investigations for ‘simple’ chemical reactions at surfaces. We have carried out such studies for the catalytic oxidation of CO at transition metal surfaces, in particular, at the ruthenium surface for which unusual behavior compared to other transition metal catalysts has been reported. High gas pressure catalytic reactor experiments have revealed that the reaction rate over Ru for oxidizing conditions is the highest of the transition metals considered — in contrast, under ultra-high vacuum conditions, the rate is by far the lowest. We find it important for understanding the pressure dependence of the reaction that Ru(0001) can support high concentrations of oxygen at the surface. Under these conditions, the O–metal bond is atypically weak compared to that at lower coverages. We have investigated a number of possible reaction pathways for CO oxidation for the conditions of high oxygen coverage, including scattering reactions of *gas-phase* CO at the oxygen covered surface (Eley–Rideal mechanism) as well as the Langmuir–Hinshelwood mechanism involving reaction between *adsorbed* CO molecules and O atoms. © 1999 Elsevier Science B.V. All rights reserved.

Keywords: Carbon monoxide; Catalysis; Density functional calculations; Oxygen; Ruthenium; Surface chemical reaction

1. Introduction

Carbon monoxide oxidation is one of the most extensively studied heterogeneous catalytic reactions. This is due to both its technological importance (e.g. in car exhaust catalytic converters where the active components are transition metals such as Pt, Pd, and Rh) and its ‘simplicity’ [1–5]. A *microscopic* understanding, however, of this most fundamental catalytic reaction is still lacking. We note, however, that steps in this direction have recently been made via first-principles calculations

[6–10]. Experimentally, it is difficult to probe the state of the reactants *during* reaction — traditionally, information is only available before or after the event. Advances in surface science techniques, however, afford new information concerning the behavior of the reactants during the reaction process. For example, time-resolved scanning tunneling microscopy (STM) [11], time-resolved electron energy-loss spectroscopy (TREELS) [12,13], time-resolved infrared spectroscopy (TRIS) [14], and (‘fast’ high resolution) X-ray photoelectron spectroscopy (XPS) [15–17]. On a larger scale are low-energy electron microscopy (LEEM) [18,19] and photoemission electron microscopy (PEEM) [20,21]. Theoretically, a significant hindrance has

^{*} Corresponding author. Fax: +49-30-8413-4701.

E-mail address: stampflc@fhi-berlin.mpg.de (C. Stampfl)

been computational limitations, but also, for a realistic description of certain reactions, new theoretical developments had to be awaited; for example, the generalized gradient approximation (GGA) for the exchange-correlation functional has been shown to be crucial for obtaining accurate activation barriers for hydrogen dissociation at metal and semiconductor surfaces [22,23].

Past studies performed using surface science techniques, i.e. on well-characterized single-crystal metal surfaces under ultra-high vacuum (UHV) conditions, have shown that CO oxidation proceeds via the Langmuir–Hinshelwood (L–H) mechanism in which reaction takes place between *chemisorbed* reagents [1–3]. Recent high gas pressure catalytic reactor experiments, which afford the study of chemical reactions under ‘realistic’ high pressure and temperature conditions, support the assignment of the L–H mechanism for Pt, Pd, Rh, and Ir [5]. For Ru, however, somewhat anomalous behavior was found which indicated that reaction via scattering of CO molecules with adsorbed O atoms may be taking place, i.e. via an Eley–Rideal type mechanism [24]. In particular, with pressures of about 10 Torr and for oxidizing conditions (i.e. at CO/O₂ pressure ratios < 1) the rate of CO₂ production was found to be significantly higher than at the other transition metal surfaces [24,25]; in contrast, under UHV conditions, the rate is extremely low over Ru(0001) [1–3,26,27]. Unlike the other transition metals, almost no chemisorbed CO could be detected either during or after the reaction, and the kinetic data (activation energy and pressure dependencies) was found to be markedly different from that of the other metals; in particular, the highest rates occurred for high concentrations of oxygen at the surface, whereas for the other metals, the highest rates occurred for low O coverages. Our studies show that Ru does behave differently from the other transition metal catalysts in that high coverages of O can be supported on the surface (up to desorption temperatures) where the O–metal bond is significantly weaker than in the lower coverage phases. Investigation of the energetics for CO₂ formation indicates that a Langmuir–Hinshelwood mechanism, rather than an Eley–Rideal process is dominant.

2. Calculation method

In order to gain an understanding of the apparently different behavior of Ru for the CO oxidation reaction, and to obtain a microscopic picture of this basic surface catalyzed reaction in general, we carried out density-functional theory (DFT) calculations ([28,29]; <http://www.fhi-berlin.mpg.de/th/fhimd.html>). We use the ab initio pseudopotential plane wave method and the supercell approach where we employ the GGA [30] for the exchange-correlation interaction. We use ab initio, fully separable, norm-conserving GGA pseudopotentials ([31,32]; <http://www.fhi-berlin.mpg.de/th/fhimd.html>), where for the Ru atoms, relativistic effects are taken into account using weighted spin-averaged pseudopotentials. The surface is modelled using a (2 × 2) surface unit cell with four layers of Ru(0001). An energy cut-off of 40 Ry is taken with three special *k*-points in the two-dimensional Brillouin zone [33]. The adsorbate structures are created on one side of the slab. We relax the position of the atoms, keeping the Ru atoms in the bottom two layers fixed at their bulk-like positions.

3. Oxygen on ruthenium

Under UHV conditions, at room temperature, dissociative adsorption of O₂ results in an (apparent) saturation coverage of $\theta_{\text{O}} \approx 1/2$, corresponding to the formation of a (2 × 1)-O structure [34]. At $\theta_{\text{O}} = 1/4$, a (2 × 2)-O phase forms [35]. Here $\theta_{\text{O}} = 1$ means that there are as many O atoms as there are Ru atoms in the top layer. In both surface structures, O adsorbs in the hexagonal close-packed (hcp) site. Our earlier DFT-GGA calculations for O on Ru(0001) [36–38] indicated that even higher coverage phases should form; namely, a (1 × 1)-O structure with coverage $\theta_{\text{O}} = 1$, as well as a (2 × 2)-3O structure with coverage $\theta_{\text{O}} = 3/4$. As for the lower coverage structures, the O atoms occupy hcp sites. The adsorption energy of O decreases notably with increasing coverage, and for the monolayer coverage phase the adsorption energy is ~ 0.7 eV less than that of the (2 × 2)-O phase. Both the (2 × 2)-3O and (1 × 1)-O structures have subsequently been cre-

ated experimentally with the use of NO_2 or high gas pressures of O_2 [38–41], and the atomic structure verified by dynamical low-energy electron diffraction (LEED) intensity analyses. NO_2 readily dissociates at elevated temperatures in the presence of adsorbed oxygen, delivering atomic oxygen to the surface while NO desorbs. Furthermore, it has been demonstrated that *after* completion of the monolayer oxygen structure, additional oxygen can enter the subsurface region [38,42] at elevated temperatures. Formation of the higher coverage phases ($\theta=3/4$ and 1.0) from gas-phase O_2 at ‘usual’ exposures under UHV conditions is apparently kinetically hindered by activation barriers for O_2 dissociation, induced by the pre-adsorbed oxygen atoms at coverage $\theta_{\text{O}} \approx 0.5$. With respect to the high pressure catalytic reactor experiments mentioned above, because the conditions under which the highest rates of CO_2 formation were reported involved high O_2 partial gas pressures and oxidizing conditions, there will be a significant attempt frequency of O_2 to overcome activation barriers for dissociative adsorption. Thus, it is likely that during reaction the oxygen coverage on the surface approaches one monolayer. We note also that in the catalytic reactor experiments may be unlikely that there is significant subsurface oxygen present since the temperature range studied in the experiment, 380–500 K, is less than the 600 K at which oxygen is reported to enter the subsurface region with an appreciable rate (using NO_2) [38,42] and Auger electron spectroscopy indicated a coverage of about one monolayer.

4. Reaction via gas-phase CO with adsorbed O

In earlier publications we reported our investigation for reaction via scattering of gas-phase CO with adsorbed O [6–8], so here we only briefly describe the results.

The $(1 \times 1)\text{-O}$ phase is assumed to cover the whole surface and we investigate the interaction of CO with this oxygen-covered surface. For a given lateral position, CO is placed well above the surface (with the C-end down) and the total energy calculated for decreasing distances of CO from the surface. All atomic positions are relaxed except

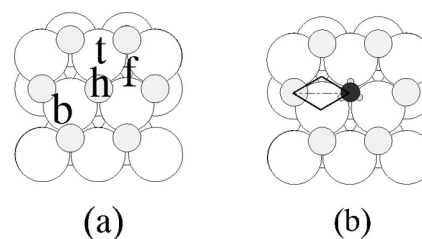


Fig. 1. (a) Schematic diagram illustrating the on-top (t), fcc (f), hcp (h), and bridge (b) sites of $(1 \times 1)\text{-O/Ru}(0001)$. Small and large circles represent O and Ru atoms, respectively. (b) Top view of CO adsorbed in an O-vacancy of $(1 \times 1)\text{-O/Ru}(0001)$. The full lines represent the (symmetry inequivalent) region within which we consider reaction takes place. CO is indicated by the small black circle.

that of the C atom which is held fixed (and the bottom two Ru layers). We considered a number of lateral positions: the on-top and fcc sites, with respect to the Ru(0001) substrate, a bridge site between two adsorbed O atoms, as well as directly above an adsorbed O(a) atom (see Fig. 1a). We find that an energy barrier begins to build up at about 2.5 \AA from the surface (with respect to the average position of the O atoms) for all sites, reflecting a *repulsive* interaction of CO with the O-covered surface. A very weak physisorption well of about 0.04 eV is also found above the O-adlayer. Its position is $\sim 3.0 \text{ \AA}$ from the surface for the on-top and fcc sites, and $\sim 3.5 \text{ \AA}$ for the bridge site and the approach directly over the O atom. Thus, for a full monolayer coverage of oxygen on the surface, CO is unable to form a chemical bond with the substrate and the L–H reaction mechanism is therefore prevented.

In order to obtain a more detailed understanding of CO_2 formation via a scattering reaction, we evaluated an appropriate cut through the high-dimensional potential energy surface (PES) (see Refs. [6–8]). This cut is defined by two variables: the vertical position of the C atom and the vertical position of the reacting O(a) adatom directly below. Initially, with the CO-axis held perpendicular to the surface, we find that the activation barrier for CO_2 formation is $\sim 1.6 \text{ eV}$. When the tilt angle of the CO-axis is allowed to relax, the energy barrier is reduced to about 1.1 eV. The transition state (depicted in the inset to Fig. 2) has a ‘bond angle’ of $\sim 131^\circ$ and the reacting O(a)

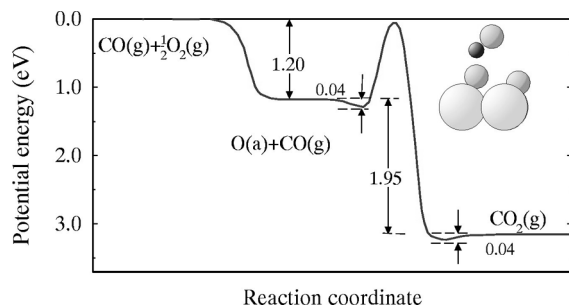


Fig. 2. Calculated energy diagram for the E-R mechanism of CO oxidation at Ru(0001). Note that the depths of the physisorption wells are exaggerated for clarity. The transition state geometry is indicated in the inset. The large, medium, and small (dark) circles represent Ru, O, and C atoms, respectively.

atom is ~ 0.35 Å above the other O atoms in the surface unit cell. The C–O(a) bond length is 1.50 Å (stretched by 27% compared to the calculated bond length of a free CO₂ molecule which is 1.18 Å; the experimental value is 1.16 Å [43]), and the bond length of CO is 1.17 Å (the calculated value of a free CO molecule is 1.15 Å; the experimental value is also 1.15 Å [43]). After onset of reaction, the CO–O(a) bond begins to develop and the O(a)–Ru bond is weakened. It then becomes energetically unfavorable for the reacting complex to be at the surface and it is strongly repelled towards the vacuum region. The resulting energy diagram is shown in Fig. 2. It can be seen that there is a significant energy gain from the surface reaction of 1.95 eV.

Using the determined activation barrier in a simple Arrhenius type equation with the prefactor obtained from consideration of the number of CO molecules hitting the surface per site per second at a given temperature and pressure, we can estimate the reaction rate [6–8]. This will give an upper bound since, for other orientations of the molecule, the barrier is larger. The rate is found to be significantly lower (by 3×10^{-6}) than that measured experimentally [25]. This indicates that this mechanism alone cannot explain the enhanced CO₂ turnover frequency, as was speculated. To investigate other possible reaction channels, we consider it conceivable that there are vacancies in the perfect (1 × 1)-O adlayer (see Refs. [6–8] for an estimate of the O-vacancy density). CO mole-

cules may then adsorb at these vacant sites and react via a L–H mechanism. In the following section we investigate such a L–H reaction mechanism.

5. Reaction between adsorbed CO and O

We first consider the energetics of adsorption of CO into a vacant hcp site of the monolayer oxygen structure. Interestingly, we find that there is an activation barrier of ~ 0.3 eV. We expect, however, that this barrier will relatively easily be overcome at the high gas pressures used in the catalytic reactor experiments. From Fig. 1b it can be seen that CO is closely surrounded by a hexagonal arrangement of six O atoms. Even though the reactants are already very close, there is still a repulsive rather than an attractive interaction between CO and the neighboring O atoms. In determining the reaction path we consider reaction in the inequivalent area of the surface, indicated in Fig. 1b by the continuous lines. There are clearly a number of possible ways that the reaction between CO and a neighboring O atom could proceed: for example, the CO molecule may approach an O atom, an O atom may approach the CO molecule, or the reactants may both move towards each other. For each of these scenarios there are obviously also a number of possible reaction paths (i.e. via the on-top site, bridge and fcc site, etc.). To determine the minimum energy pathway, energy barrier, and associated transition state, is clearly not a simple problem. Recent ab initio studies of surface reactions and dissociation of diatomic molecules at surfaces have attempted ‘direct methods’ to find the lowest energy reaction pathway [10,44]. In the present work, however, we use the ‘standard grid approach’ of constructing various relevant PESs, since we are also interested in the *shape* of the PES away from the minimum energy reaction pathway.

In view of the weaker CO–metal bond strength compared to that of the O–metal bond strength at this coverage, i.e. 0.85 eV compared to 2.09 eV (with respect to gas phase $\frac{1}{2}$ O₂), we first consider reaction via movement of CO towards the O atom.

This in fact turns out to have the lowest energy pathway of those we considered with a barrier of ~ 1.51 eV. This value is consistent with the recent experimental estimate of >1.4 eV for the case of high oxygen coverages on the surface [45]. Other possible reaction pathways considered were for O to move towards CO and for O and CO to move towards each other over one Ru atom. The lowest energy pathways found for these scenarios were at least 0.2 and 0.3 eV higher, respectively. We point out that in this work we have only considered the most obvious reaction paths, and in order to explore in more detail the very complex nature of this high-dimensional potential energy surface, further calculations are required.

As a first step we investigate the energetics for different fixed lateral positions of the C atom within the area shown in Fig. 1b. We initially keep the lateral position of the O atoms fixed, but allow vertical relaxations. For CO moving towards the on-top site (see Fig. 1), a strong repulsion between C and the two symmetrically equivalent O atoms develops giving rise to a large energy barrier of 2.53 eV. Thus, the pathway over the on-top site is energetically unfavorable.

Interestingly, the situation is somewhat different for CO moving towards the fcc site: in this direction there is also the build up of an energy barrier; on overcoming the barrier, however, there is an *attractive* interaction between C and the *two* symmetrically equivalent O atoms (see Fig. 1b). When the O atoms are then allowed to laterally relax, we find the formation of a carbonate-like species. The atomic geometry is depicted in Fig. 3a. We note that in our investigations of the CO-gas scattering reaction, we also identified the stability of such a carbonate species on the fully O-covered surface; the atomic geometry is similar as can be seen from Fig. 3b. Formation of this species was also found to involve a significant energy barrier. We note that experimental identification of carbonate species in CO oxidation reactions over other transition metals has been reported (e.g. Ref. [46]), where they may possibly act as an intermediary. The actual role they play in the carbon monoxide oxidation reaction for this system, however, is at present unknown.

We find that the minimum energy pathway found for CO₂ formation corresponds to one where

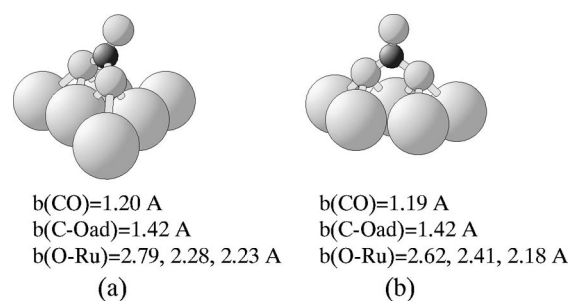


Fig. 3. Atomic geometry of identified carbonate species at (a) a vacancy in the monolayer oxygen structure, and (b) at the perfect (1×1) -O/Ru(0001) surface. The large, small, and small dark circles represent Ru, O, and C atoms, respectively. The various bond lengths are indicated (in Å).

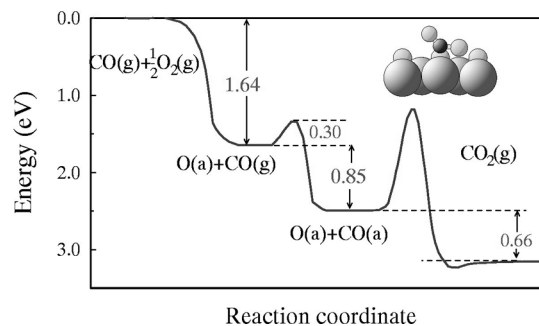


Fig. 4. Calculated energy diagram for the L–H mechanism of CO oxidation at Ru(0001). The transition state geometry is indicated in the inset. The large, small, and small darker circles represent Ru, O, and C atoms, respectively.

the CO molecule moves essentially directly towards the O atom. The associated energetics are shown in Fig. 4 where we have constructed the energy diagram. (We point out that allowing lateral atomic relaxations of the neighboring O atoms during determination of the reaction pathway may lead to a slightly lower energy barrier for CO₂ formation.) Similarly to our study of the E–R mechanism, we also find a small physisorption well for CO₂ above the surface. The corresponding transition state geometry is depicted in the inset of Fig. 4. In this geometry, the C–O(a) bond is almost parallel to the surface and the CO axis is bent away from O(a) yielding a bent CO–O(a) complex with a bond angle of 125° , similar to that found for the E–R mechanism. The C–O(a) bond length is 1.59 Å (about 35% stretched compared

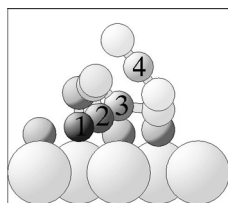


Fig. 5. Atomic positions at selected points along the reaction energy pathway CO_2 formation. The large, small, and small darker circles represent Ru, O, and C atoms, respectively.

to that in CO_2) and the CO bond length is 1.18 Å. Fig. 5 shows the atomic geometry at selected positions along the reaction path to CO_2 formation. Initially CO is in the vacancy and O(a) in the hcp site. As CO approaches O(a), repulsive forces build up on both the C and O(a) atoms and the molecular axis of CO begins to tilt away from O(a). At the transition state, CO and O begin to lift off the surface as they break their metal bonds in favor of developing a C–O(a) bond. Interestingly, the distance that O moves away from the surface is ~ 0.36 Å; very similar to that found in the E–R mechanism which was ~ 0.35 Å. As CO_2 begins to form, the molecular axis quickly straightens out to its linear geometry.

The corresponding valence electron density and density difference distributions are shown in Fig. 6. The latter is constructed by subtracting from the electron density of the CO,O/Ru(0001) system those of the O-covered surface and a free CO molecule. From the electron density difference distributions, with respect to the starting configuration of CO in the vacancy, it can be seen that as CO moves towards O(a), firstly there is less electron density in the CO $2\pi^*$ orbitals, indicating a weakening of the C–metal bond. Also, electron density has been depleted from the O(a) orbital pointing towards the CO molecule and an increase occurs into orbitals in the orthogonal direction (pointing in a near-perpendicular direction to the surface). The redistribution is an effect of Pauli repulsion. At the transition state, the onset of bond formation can be seen between these latter O(a) orbitals and the $2\pi^*$ -like orbitals of the C atom. We can notice that CO is bonded only weakly to the metal through a $2\pi^*$ -like orbital. The bond of the reacting O(a) to the surface is also

significantly weakened at the transition state as can be seen from the lower panel showing the total valence electron density. Interestingly, the density difference plot for the transition state is very similar to that of the E–R process (see fig. 7 of Ref. [7]). In the last panel (leftmost), significant accumulation of electron density can be seen between the C and O(a) atoms as the CO_2 molecule is practically formed.

To summarize, our studies indicate that a Langmuir–Hinshelwood mechanism rather than an Eley–Rideal mechanism is the *dominant* reaction process giving rise to the reported increase in reactivity of ruthenium for the CO oxidation reaction as measured in the high pressure catalytic reactor experiments as compared to under UHV conditions. We find that for high coverages of O on the surface, which are attainable under the sufficiently high oxygen pressures used in the experiment, the O adsorption energy is notably weaker than the lower coverage phases that form under UHV conditions. Furthermore, the adsorption energy of CO in the presence of high O coverages is weaker than in the presence of low O coverages. These factors, together with the close proximity of the reactants, is thought to give rise to the observed increase in reactivity of Ru and the reported anomalous behavior on partial gas pressure.

Finally, we would like to mention some very recent results of CO oxidation experiments. For the case of very high concentrations of oxygen at the surface (one monolayer on the surface plus oxygen occupying *subsurface* sites) which can be prepared after formation of the (1×1) phase by using either NO_2 or high gas pressures of O_2 at *elevated* temperatures, reaction rates notably greater than that from the on-surface monolayer oxygen structure have been measured [45,47]. These high rates have been proposed to be connected to the existence of copious amounts of oxygen in the subsurface region. These are clearly very interesting results and require more detailed investigations in order to understand this behavior.

6. Conclusion

We have performed density functional theory calculations in order to investigate the catalytic

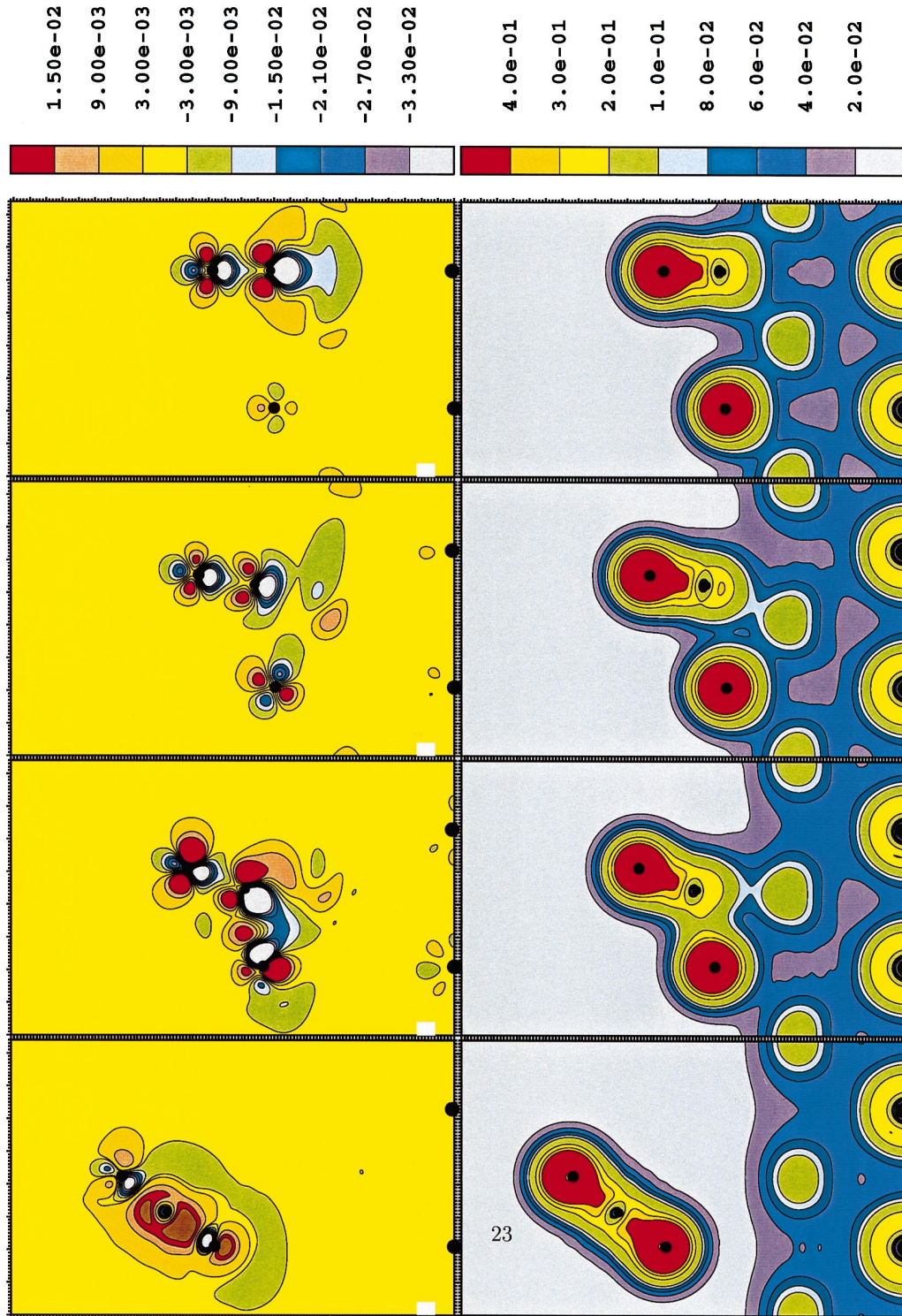


Fig. 6. Valence electron density (lower panels) and density difference distributions (upper panels) for selected positions along the reaction path. The units are $e \text{ bohr}^{-3}$. For the upper leftmost panel the contours differ: the first negative contour is -3×10^{-3} and the spacing is 15×10^{-3} and the first positive contour is at 3×10^{-3} and the spacing is 30×10^{-3} .

oxidation of carbon monoxide over Ru(0001) for the conditions of high oxygen coverage on the surface for which highest reaction rates of CO₂ formation have been reported. It is only by exposure of the surface to high O₂ gas pressures, or with the use of strongly oxidative molecules such as NO₂, that high oxygen coverages can be achieved. In this case the O–metal bond strength is notably weaker compared to the lower coverage structures that form under UHV conditions, and as such is expected to be more reactive. In the present work we concentrated mainly on the microscopic description and study of the Langmuir–Hinshelwood reaction mechanism. We identified a bent transition state for CO movement towards an adsorbed O atom with an associated energy barrier of approximately 1.5 eV. In this configuration the CO and the adsorbed O atom have substantially weakened (and significantly stretched) their bond to the substrate.

References

- [1] T. Engel, G. Ertl, *J. Chem. Phys.* 69 (1978) 1267.
- [2] T. Engel, G. Ertl, *Adv. Catal.* 28 (1979) 1.
- [3] D.A. King, D.P. Woodruff (Eds.), *The Chemical Physics of Solid Surfaces and Heterogeneous Catalysis*, Vol. 4, Elsevier, Amsterdam, 1982.
- [4] A. Bielanski, J. Haber, in: H. Heinemann (Ed.), *Oxygen in Catalysis*, Marcel Dekker, New York, 1991, Chapter 6.
- [5] C.H.F. Peden, in: D.J. Dwyer, F.M. Hoffmann (Eds.), *Surface Science of Catalysis: In situ Probes and Reaction Kinetics*, American Chemical Society, Washington, DC, 1992.
- [6] C. Stampfl, M. Scheffler, *Phys. Rev. Lett.* 78 (1997) 1500.
- [7] C. Stampfl, M. Scheffler, *J. Vac. Sci. Technol. A* 15 (1997) 1635.
- [8] C. Stampfl, M. Scheffler, *Surf. Sci.* 377–379 (1997) 808.
- [9] A. Alavi, P. Hu, T. Deutsch, P.L. Silvestrelli, J. Hutter, *Phys. Rev. Lett.* 80 (1998) 3650.
- [10] A. Eichler, Ph.D. Thesis, Technical University of Vienna, January 1998.
- [11] J. Wintterlin, S. Völkening, T.V.W. Janssens, T. Zambelli, G. Ertl, *Science* 278 (1997) 1931, and references cited therein.
- [12] W. Ho, *J. Vac. Sci. Technol. A* 3 (1985) 1432.
- [13] L.H. Dubois, T.H. Ellis, S.D. Kevan, *J. Vac. Sci. Technol. A* 4 (1985) 1505.
- [14] J.E. Reutt-Robey, D.J. Doren, Y.J. Chabal, S.B. Christman, *Phys. Rev. Lett.* 61 (1998) 2778.
- [15] A. Baraldi, G. Comelli, S. Lizzit, D. Cocco, G. Paolucci, R. Rosei, *Surf. Sci.* 367 (1996) L67.
- [16] G. Comelli, A. Baraldi, S. Lizzit, D. Cocco, G. Paolucci, R. Rosei, M. Kiskinova, *Chem. Phys. Lett.* 261 (1996) 253.
- [17] P.D. Cobden, B.E. Nieuwenhuys, F. Esch, A. Baraldi, G. Comelli, S. Lizzit, M. Kiskinova, *J. Vac. Sci. Technol. A* 16 (1998) 1014.
- [18] W. Telieps, E. Bauer, *Ultramicroscopy* 17 (1985) 57.
- [19] K.C. Rose, B. Berton, R. Imbihl, W. Engel, A.M. Bradshaw, 79 (1997) 3427.
- [20] R. Imbihl, G. Ertl, *Chem. Rev.* 95 (1995) 697.
- [21] H.H. Rottermund, *Surf. Sci. Rep.* 29 (1997) 265.
- [22] B. Hammer, K.W. Jacobsen, J.K. Nørskov, *Phys. Rev. Lett.* 70 (1993) 3971.
- [23] B. Hammer, M. Scheffler, K.W. Jacobsen, J.K. Nørskov, *Phys. Rev. Lett.* 73 (1994) 1400.
- [24] C.H.F. Peden, D.W. Goodman, M.D. Weisel, F.M. Hoffmann, *Surf. Sci.* 253 (1991) 44.
- [25] C.H.F. Peden, D.W. Goodman, *J. Phys. Chem.* 90 (1986) 1360.
- [26] H.-I. Lee, J.M. White, *J. Catal.* 63 (1980) 261.
- [27] V.I. Savchenko, G.K. Borekov, A.V. Kalinkin, A.N. Salanov, *Kinet. Catal.* 24 (1984) 983.
- [28] R. Stumpf, M. Scheffler, *Comp. Phys. Commun.* 79 (1994) 447.
- [29] M. Bockstedte, A. Kley, J. Neugebauer, M. Scheffler, *Comp. Phys. Commun.* 107 (1997) 187.
- [30] J.P. Perdew, J.A. Chevary, S.H. Vosko, K.A. Jackson, M.R. Pederson, D.J. Singh, C. Fiolhais, *Phys. Rev. B* 46 (1992) 6671.
- [31] N. Troullier, J.L. Martins, *Phys. Rev. B* 43 (1993) 1991.
- [32] M. Fuchs, M. Scheffler, *Comp. Phys. Commun.*, in press.
- [33] S.L. Cunningham, *Phys. Rev. B* 10 (1974) 4988.
- [34] H. Pfnür, G. Held, M. Lindroos, D. Menzel, *Surf. Sci.* 220 (1989) 43.
- [35] M. Lindroos, H. Pfnür, G. Held, D. Menzel, *Surf. Sci.* 222 (1989) 451.
- [36] C. Stampfl, M. Scheffler, *Phys. Rev. B* 54 (1996) 2868.
- [37] C. Stampfl, *Surf. Rev. Lett.* 3 (1996) 1567.
- [38] C. Stampfl, S. Schwegmann, H. Over, M. Scheffler, G. Ertl, *Phys. Rev. Lett.* 77 (1996) 3371.
- [39] K.L. Kostov, M. Gsell, P. Jakob, T. Moritz, W. Widdra, D. Menzel, *Surf. Sci.* 394 (1997) L138.
- [40] Y.D. Kim, S. Wendt, S. Schwegmann, H. Over, G. Ertl, in preparation.
- [41] M. Gsell, M. Stichler, P. Jakob, D. Menzel, *Israel J. Chem.*, in press.
- [42] W.J. Mitchell, W.H. Weinberg, *J. Chem. Phys.* 104 (1996) 9127.
- [43] B.G. Johnson, P.M.W. Gill, J.A. Pople, *J. Chem. Phys.* 98 (1993) 5612.
- [44] J.J. Mortensen, B. Hammer, J.K. Nørskov, *Phys. Rev. Lett.* 80 (1998) 4333.
- [45] A. Böttcher, H. Niehus, S. Schwegmann, H. Over, G. Ertl, *J. Phys. Chem.* 101 (1997) 11185.
- [46] C.H.F. Peden, J.E. Houston, *J. Catal.* 128 (1990) 405.
- [47] A. Böttcher, H. Niehus, submitted to *Phys. Rev. B*.